In-Bore Projectile Dynamics in the Linear Induction Launcher (LIL)
Part I: Oscillations

Ki-Bong Kim, Zivan Zabar, Enrico Levi and Leo Birenbaum
Polytechnic University, 333 Jay St., Brooklyn, NY 11201

Abstract: The projectile in a linear induction launcher is subject to centering (levitation) forces, as well as propelling ones. Due to their uneven distribution, these forces give rise to rotation, as well as translation of the projectile axis. This paper assesses these motions.

1. Introduction

This paper deals with the analysis of the projectile stability in a linear induction launcher (LIL), which is an induction type coil-gun. In particular, it is focused on coil-guns driven by generators or by capacitors [1,2]. In either case, the input energy is delivered when a switch is closed. Since the coil-gun is a hyper-velocity machine and the transit time of the projectile within the barrel is in the order of milliseconds, the transient performance is dominant. The problem of projectile stability arises since the projectile of the LIL is supported only by air and by electromagnetic forces, but not by any other physical means. It is possible that the projectile of the LIL can find itself offset from the axis of the barrel because of initial position or mechanical disturbance during the travel. In this case, the projectile must be restored to a coaxial situation without touching the walls of the barrel. This analysis starts with the assumption that the projectile is initially offset by unknown reasons; the dynamic motions of the projectile in the barrel are then analyzed to see if the restoration process of the projectile is satisfactory.

2. Restoring Force in the Projectile

For the purpose of analysis in terms of lumped circuit parameters, the projectile, which is a continuous, finite length cylindrical tube or sleeve, is assumed to consist of a finite number of discrete sleeve coils. As a result, the continuous restoring force which is exerted on the projectile in the coil-gun when it is offset for any reason, is also discretized as a number of separate forces, each acting on one sleeve coil. Since the barrel of the coil-gun also consists of a number of coils, each sleeve coil is acted upon by all the drive coils. Thus, the coil-gun is reduced to a multi-drive-coil and multi-sleeve-coil system.

Let us consider Fig. 1, and let N_{dc} and N_{pc} be the numbers of coils of the driving barrel and of the passive projectile sleeve, respectively.

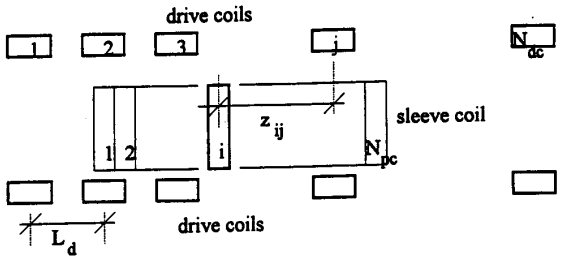

Fig. 1: Multi-coil sleeve and multi-coil barrel

The restoring force acting upon each sleeve coil is the algebraic sum of the effects of all the drive coils. Defining the unit restoring force F_{su} as the force per unit turn and unit ampere, and assuming that each coil consists of a single filament, the restoring force F_{si} acting on each coil of the projectile sleeve can be expressed in matrix form [3] as Eq. 1.

The general equation for the unit restoring force function used above is

$$F_{su.ij} = \frac{\mu_0 R_p}{2\pi} \int_{-\pi/2}^{\pi/2} [G_{1ij} - G_{2ij}]\, d\phi_1 \qquad \text{N/A}^2 \qquad (2)$$

for $i = 1, \ldots\ldots, N_{pc}$ and $j = 1, \ldots\ldots, N_{dc}$; where

$$G_{kij} = \left(\frac{R_d^2 - r_k^2 - z_{ij}^2}{(R_d - r_k)^2 + z_{ij}^2} E_{kij} + K_{kij} \right) \frac{\cos\phi_2}{\sqrt{(R_d + r_k)^2 + z_{ij}^2}}$$

$k = 1, 2$. Refers to coordinate systems of drive and projectile coils, respectively.

ϕ_1, r_1 = angular, radial coordinates of a point on the projectile coil, in the drive coil coordinate system

ϕ_2, r_2 = angular, radial coordinates of the same point on the projectile coil, in the projectile coil coordinate system

$z_{ij} = z + L_p(i-1) - L_d(j-1)$

z = distance between the first drive coil and the first sleeve coil at a certain time

L_d ; L_p = distance between two drive coils; between two projectile coils

(1)
$$\begin{bmatrix} F_{s1} \\ F_{s2} \\ \vdots \\ F_{sN_{pc}} \end{bmatrix} = \begin{bmatrix} I_{p1}\, n_{p1} & 0 & \cdots & 0 \\ 0 & I_{p2}\, n_{p2} & \cdots & 0 \\ \vdots & \vdots & \ddots & \vdots \\ 0 & 0 & \cdots & I_{pN_{pc}}\, n_{pN_{pc}} \end{bmatrix} \begin{bmatrix} F_{su11} & F_{su12} & \cdots & F_{su1N_{dc}} \\ F_{su21} & F_{su22} & \cdots & F_{su2N_{dc}} \\ \vdots & \vdots & \ddots & \vdots \\ F_{suN_{pc}1} & F_{suN_{pc}2} & \cdots & F_{suN_{pc}N_{dc}} \end{bmatrix} \begin{bmatrix} I_{d1}\, n_{d1} \\ I_{d2}\, n_{d2} \\ \vdots \\ I_{dN_{dc}}\, n_{dN_{dc}} \end{bmatrix}$$

n_{dj}; n_{pi} = turns of j^{th} drive coil; of i^{th} projectile coil

R_d; R_p = radius of drive coil; of projectile coil

Manuscript received May 1, 1994
This work was sponsored by the BMDO/IST and managed by US Army SDC under contract DASG60-91-C-015

$$E_{kij} = \int_{-\pi/2}^{\pi/2} \sqrt{1 - \kappa_{kij}^2 \sin^2(\vartheta)}\, d\vartheta \quad ; \quad k = 1, 2$$

$$K_{kij} = \int_{0}^{\pi/2} \frac{1}{\sqrt{1 - \kappa_{kij}^2 \sin^2(\vartheta)}}\, d\vartheta \quad ; \quad k = 1, 2$$

$$\kappa_{kij}^2 = \frac{4 R_d r_k}{(R_d + r_k)^2 + z_{ij}^2} \quad ; \qquad k = 1, 2$$

The force expressed in Eq. (1) is the restoring force for the i^{th} sleeve coil due to the N_{dc} drive coils.

The analysis of the projectile motion is facilitated if, instead of the forces on each coil, one considers an equivalent system consisting of one or two forces only. The necessary and sufficient conditions for two systems of forces a and b to be equivalent are $\sum_{i=1}^{n} F_{ai} = \sum_{j=1}^{m} F_{bj}$ and $\sum_{i=1}^{n} M_{ai} = \sum_{j=1}^{m} M_{bj}$ where F is force and M is moment or torque [4].

3. Trajectory of the Projectile Tail and Head

The overall dynamic motion is the result of a linear motion and a rotational motion. The two governing equations for these motions are :

$$F(t) = ma(t) + \lambda v(t) = m \frac{d^2 y(t)}{dt^2} + \lambda \frac{dy(t)}{dt} \tag{3}$$

$$T(t) = J\alpha(t) + B\omega(t) = J \frac{d^2 \vartheta(t)}{dt^2} + B \frac{d\vartheta(t)}{dt} \tag{4}$$

where F is the equivalent force found by the method described in section (2); $y(t)$ is the displacement, due to translation, in the radial direction; T is the torque (or moment) about the mass center; $\vartheta(t)$ is the angle between the axes of the projectile and the barrel; J is the moment of inertia of the projectile about its center of mass; $\omega(t)$ and $a(t)$ are the angular velocity and angular acceleration of the projectile about its center of mass; λ and B are the viscous friction coefficients for linear and for rotational motion.

Equations (3) and (4) relate to linear translation and to rotation, respectively.

The trajectories of the tail and head of the projectile can be obtained by solving these two dynamic equations. The solution for the trajectory of the tail is:

$$y_{tail}(t) = \left[\frac{1}{\lambda} F(t)^* \left(1 - e^{-\frac{\lambda}{m}t}\right) + \frac{L}{2B} T_{tail}(t)^* \left(1 - e^{-\frac{B}{J}t}\right) + y_{tail}(0)\right] U(t) \tag{5}$$

Similarly, the trajectory of the head is

$$y_{head}(t) = \left[\frac{1}{\lambda} F(t)^* \left(1 - e^{-\frac{\lambda}{m}t}\right) - \frac{L}{2B} T_{head}(t)^* \left(1 - e^{-\frac{B}{J}t}\right) + y_{head}(0)\right] U(t) \tag{6}$$

In Eqs. (5) and (6), the symbol * denotes a convolution integral; the first terms correspond to the linear translation; and the second terms correspond to the translation due to the rotation. $U(t)$ is the unit step function.

4. Distribution of Restoring Force in Projectile

As an example, numerical calculations were made for the capacitor-driven Model 3, a 500 m/s LIL designed, fabricated, and tested at the Polytechnic [5]. Its projectile consists of an aluminum sleeve 20 cm long and weighing 137 grams that is assumed to consist of 20 coils, each having 1 cm width. The barrel consists of 18 coils energized by a capacitor bank in polyphase fashion, so as to create a traveling wave of pole pitch τ = 10 cm. The barrel is divided into two sections, the first having the same length as the sleeve projectile (20 cm), and the second being 40 cm long. The second section carries currents at a higher frequency f than the first, so that the exciting wave travels at a higher velocity $v_s = 2\tau f$. Initially (at time t = 0) the sleeve is located so that the middle of the tail coil is 1 cm ahead of the middle of phase A coil. As a result, 2.25 cm of the sleeve, at its head, is outside the first section of the barrel. The first phase (phase A) of the second section is energized only after the entire sleeve has exited the first section, so that a large portion of the sleeve is outside the energized (first) portion of the barrel and, therefore, is not subject to a restoring force. It is assumed that at t = 0, the projectile rests at the bottom of the barrel (y = 1 mm, ϑ = 0). The distribution of the restoring force per coil F_s at the time 0.037 msec, when only phase A is energized, is shown in Fig. 2. The force peaks in correspondence with the location of coil –A, which is one pole pitch ahead of phase A coil.

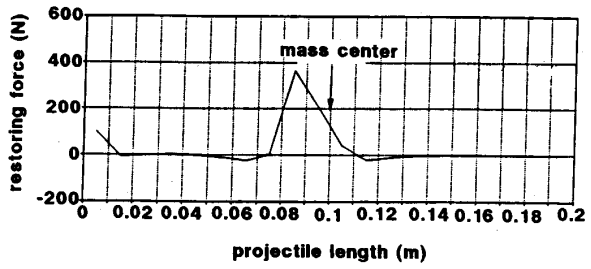

Fig. 2: Distribution of F_s along the projectile at t = 0.037 ms

It is seen that the electromagnetic force is so strong that the force of gravity (about 1.35 N) can be neglected.

The preponderance of the force on the left of the center of mass causes a clockwise rotation of the sleeve which attains the position shown in Fig. 3. Note that, for the sake of clarity, in the drawing the vertical displacement y of the projectile has been enlarged out of proportion.

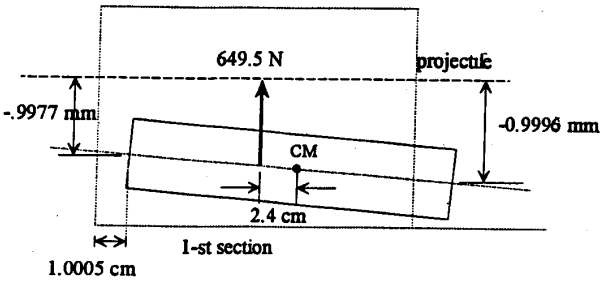

Fig. 3: Position of the projectile at t = 0.037 ms

At time t = 0.469 msec, after all the three phases of the first barrel section have been energized, the force distribution has changed as shown in Fig. 4. As a result, the projectile has acquired the position shown in Fig. 5. Note that a significant portion of the projectile (2.86 cm) is outside the energized first section and, therefore, as seen in Fig. 4 practically no force is acting on the head portion. This causes F_{eq} to push the tail of the projectile downwards even though the head is higher than the tail and, as a result, the tail vibrates with larger amplitude than the head as it travels through the first section.

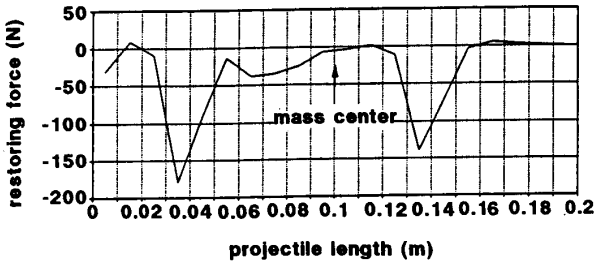

Fig. 4: Distribution of F_s along the projectile at t = 0.469 ms

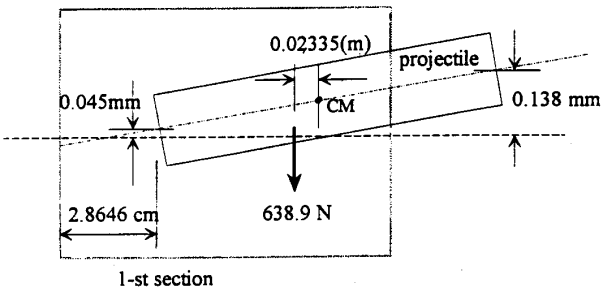

Fig. 5: Position of the projectile at t = 0.469 ms

At the time t = 1.878 msec, all three phases in the second section have been energized and the entire length of the projectile is within the second section of the barrel and is subjected to restoring forces. As shown in Figs. 6 and 7, F_{eq} is acting on the left side of the projectile pushing the tail upwards when it is lower than the head. Thus, the projectile tends to restore its position parallel to the barrel axis and this is the ideal situation.

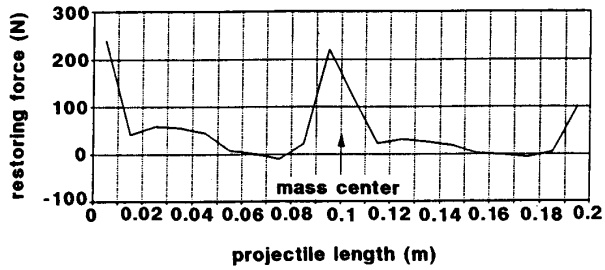

Fig. 6: Distribution of F_s along the projectile at t = 1.878 ms

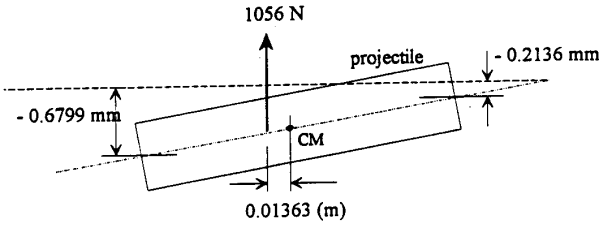

Fig. 7: Position of the projectile at t = 1.878 ms

At the time t = 2.347 msec, the restoring forces and the position of the projectile are as shown in Figs. 8 and 9.

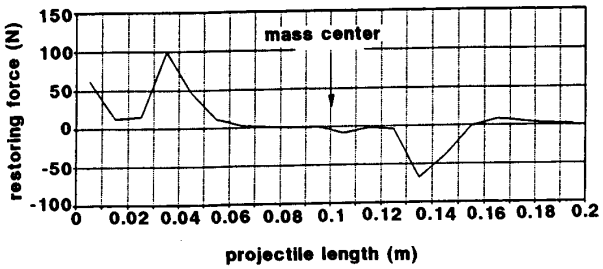

Fig. 8: Distribution of F_s along the projectile at t = 2.347 ms

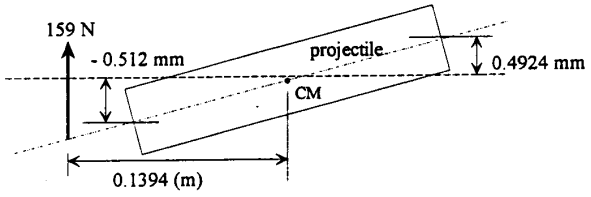

Fig. 9: Position of the projectile at t = 2.347 ms

When Figs. 7 and 9 are compared, one can notice that the projectile is more oblique in Fig. 9. Therefore, to return to a balanced position, the projectile needs faster clockwise rotation about the mass center. As shown in Fig. 9, the force is acting further outward than in Fig. 7 and this should yield a larger torque as desired. However, since much time has elapsed, the currents are much attenuated and most of the sleeve is outside the energized portion of the barrel; the magnitude of the force is much smaller than in Fig. 7.

5. Characteristics of the oscillation

For the purpose of investigating the characteristics of the oscillation, the transverse axes of the sleeve and drive coils are assumed to coincide, as seen in Fig. 10. In this case, there is no propelling force and the sleeve coil will oscillate

only in the transverse direction. Therefore, in the absence of rotation, the motion of the sleeve coil can be expressed by the linear translation equation only (Eq. 3).

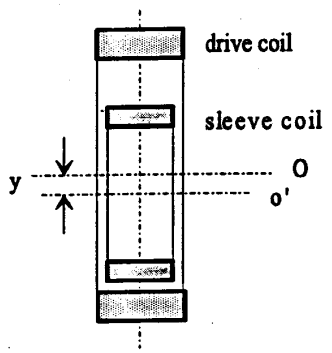

Fig. 10: Oscillation of the sleeve coil

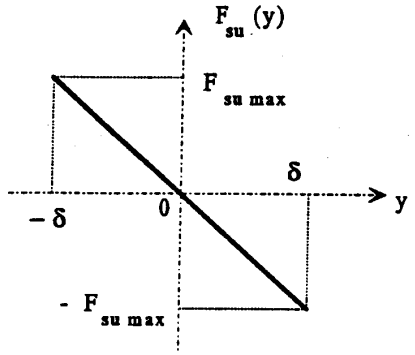

Fig. 11: Unit force characteristics

The restoring force can be expressed simply by

$$F_s(t,y) = n_d n_p I_d(t) I_p(t) F_{su}(y) \tag{7}$$

where I_d, I_p and n_d, n_p are the currents and the number of turns in the drive coil and sleeve coil, and F_{su} is the unit restoring force. The characteristic of the unit restoring force, $F_{su}(y)$, as a function of offset distance, y, is very nearly linear as shown in Fig. 11 [3]. Therefore:

$$\begin{aligned} F_s(t) &= -\frac{AB}{2} e^{-(\alpha_1+\alpha_2)t}\left(1-\cos 2\omega_o t\right)\frac{F_{su\,max}}{\delta} y(t) \\ &= -Ce^{-\alpha_3 t}\left(1-\cos 2\omega_o t\right)\frac{F_{su\,max}}{\delta} y(t) \end{aligned} \tag{8}$$

Assuming no mechanical friction in the movement of the sleeve coil, the dynamic equation in this case can be written as

$$\frac{d^2y(t)}{dt^2} + \frac{F_{smax}}{2m\delta} e^{-\alpha_3 t}\left(1-\cos 2\omega_o t\right) y(t) = 0 \tag{9}$$

The solution of this equation is a growing oscillation. However, the transit time of the projectile in the Model 3 LIL (2.4 msec) is too short to demonstrate this characteristic. Therefore, unrealistic parameter values will be used as an example. The result of such a numerical analysis, when A = 10,000, B = 1,000, $\omega_o = 2\pi \times 2{,}000$, α_3 = 8.5, δ = 1 mm, is shown in Fig. 12.

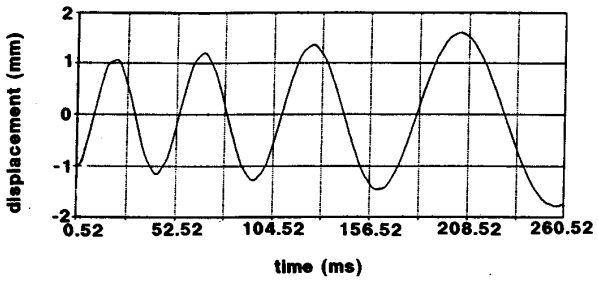

Fig. 12: Trajectory with decaying drive currents

It is important to note from Fig. 12 that the trajectory of the projectile is not a bounded oscillation.

6. Simulation

The operation of the two-section EML-3 is simulated with the following input data.

Air gap clearance is 1 mm. The initial positions of tail and head of the projectile are both $y = -1$ mm, which means that the projectile is located at the bottom of the barrel. Initially, the projectile is located 1 cm ahead of the first coil of the barrel. The initial capacitor voltage is 3.8 kV for the 1st section and 15 kV for the second section. The drive coils are fired with a firing angle of 60° in the sequence A → –C → B → –A → C → –B. Phase A in the second section is fired 1.4 msec after phase A of the first section has been fired.

The restoring force as a function of time is shown in Fig. 13.

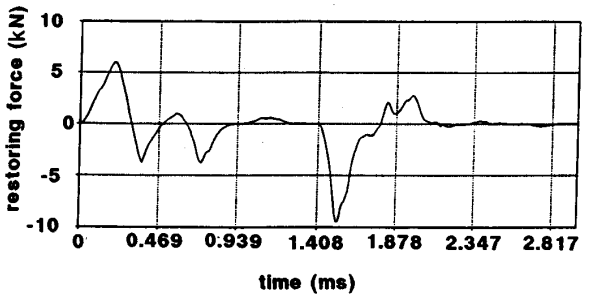

Fig. 13: Restoring force, $F_{eq}(t)$.

The restoring force curve represents the equivalent force that has been reduced from 20 coil forces in the projectile to a single equivalent force. It can be seen that the restoring force has two peaks corresponding to the energization of the first and second section respectively and that it decays rapidly thereafter.

The relation between the restoring force and the location of the mass center is plotted in Fig. 14.

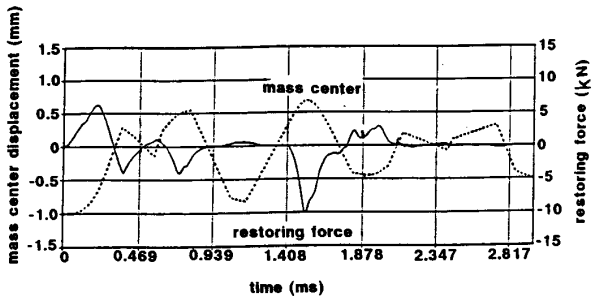

Fig. 14: Restoring force and *y* displacement of the mass center

From this figure it can be seen that the direction of the restoring force is almost opposite to the displacement of the mass center. When the mass center is located above the axis of the barrel the restoring force is directed downward so that it tends to push the projectile down. Vice versa, when the mass center is located below the axis of the barrel, the restoring force is directed upward so that it tends to push the projectile up. Since the restoring force is acting in a direction opposite to that of the projectile displacement from the barrel axis, and the motion is governed by a dynamic equation (a second order differential equation), the transverse trajectory of the projectile is an oscillation.

7. Concluding comments

A method for analyzing the off-axis motions of a cylindrical projectile in a linear induction launcher has been presented. It was applied to one particular launcher (Model 3 LIL) for which an experimental prototype exists at the Polytechnic. The transverse forces acting on the projectile tend to restore it to its (desired) on-axis location during flight, but their distribution along the projectile is not uniform. This gives rise to rotational motions.

The decay with time of the currents in the barrel and projectile causes a strong decay of the restoring force that keeps the projectile centered in the barrel. Since this force is smaller in the decelerating phase of the oscillation than in the accelerating one, the amplitude of the oscillation increases with time. This instability may cause the projectile to touch the wall of the barrel, albeit with small momentum impact. If, however, the period of the transverse oscillation exceeds the transit time by an order of magnitude, or more, then this instability may not be a significant factor. We suspect that this is indeed the case, since there has been no evidence to date in any of our experiments with the Model 3 LIL that the projectile touches the inner barrel wall. It is noted that the Model 3 LIL is characterized by a very strong damping of the currents. Experiments conducted at the ET&D (Electronics Technology and Devices) Laboratory in Fort Monmouth, NJ have shown that the cause is the strongly lossy nature of the capacitors. Their replacement with aluminum foil, polypropylene insulation capacitors would reduce not only the damping, but also the transit time of the projectile in the barrel, thus reducing the likelihood that the projectile would touch the wall of the barrel.

A companion paper discusses balloting, spinning and nutation aspects of the in-bore projectile dynamics.

Acknowledgment

This work is part of Dr. Kim's's dissertation for his Ph.D. degree in electrical engineering. This analysis is based on the Linear Induction Launcher Model-1 and Model-3 developed and built at the Polytechnic University, Brooklyn, New York. The project is sponsored by SDIO/IST and managed by USA SDC under contract DASG 60-91-C-0154.

References

[1] J. L. He, E. Levi, Z. Zabar and L. Birenbaum, "Equivalent Circuits and Parameters for Induction Type Electromagnetic Launchers", IEEE Trans. on Magnetics, Jan. 1993, Vol. 29, No. 1, pp. 667-674.

[2] J. L. He, "Analysis and Design of EM Coil Launcher", Ph.D. dissertation, Polytechnic University, June 1990.

[3] Ki-Bong Kim, "Analysis of the Projectile Stability in the Linear Induction Type Electromagnetic Launcher", Ph.D. dissertation, Polytechnic University, June 1993.

[4] F. P. Beer and R. Johnston, Jr., "Vector Mechanics for Engineers, Statics and Dynamics", 3rd edition, McGraw-Hill, 1977.

[5] Z. Zabar, X. N. Lu, E. Levi and L. Birenbaum, "Experimental Results and Performance Analysis of a 500 m/s Linear Induction Launcher (LIL)", Proc. 7th Symposium on Electromagnetic Launch Technology, April 20-24, 1994, San Diego, California.